Chapter 5
Magnetic Materials

Louis L. Reginato

5.1 Introduction

The magnetic material is a key element of the induction accelerator cell. The choice of material will generally involve a number of trade offs. Desirable properties of magnetic materials include high flux density (B_s), low coercive force (H_c), high permeability (μ), and low loss at high rates of magnetization ($\mathrm{d}B/\mathrm{d}t$), but any given application will emphasize some of these properties at the expense of the others. The acceleration gradient, pulse duration, and integration of focusing systems in the cell design place constraints on the cell aspect ratio such as the outside/inside radii. Further constraints are imposed by the limits of the modulator on parameters such as repetition rate, peak power, and rise time. Finally the budgetary constraints, particularly when several hundred tonnes of magnetic materials are required, must be included in the tradeoffs.

A large variety of ferrimagnetic (see Sects. 3.6 and 3.7) and ferromagnetic materials are available to cover induction cell designs with pulse durations from nanoseconds to microseconds. The application of ferrimagnetic materials such as ferrites and ferromagnetic materials such as silicon steel, nickel iron and amorphous magnetic materials in short- and long-pulse accelerator designs will be discussed in this chapter.

5.2 Ferrites

Ferrites are an essential class of magnetic materials used extensively in linear and nonlinear microwave applications. The application of ferrites for the induction cells in the electron ring accelerator (ERA) in the early 1970s to produce 30 ns pulses at high currents was quite novel [1]. At that time, the large diameter toroids could not be pressed as a unit so they were made by gluing bricks together to achieve the

L.L. Reginato (✉)
Lawrence Berkeley National Laboratory, Berkeley, CA 94720–8201, USA
e-mail: LLReginato@lbl.gov

K. Takayama, R.J. Briggs (eds.), *Induction Accelerators*, Particle Acceleration and Detection, DOI 10.1007/978-3-642-13917-8_5,

desired diameter. Subsequent continued development provided better materials and toroids of over one meter in diameter.

The ferrite properties of particular interest to short-pulse accelerators are their high resistivity (ρ) and moderately high permeability (μ_r) at high frequencies (short pulse). A ferrite toroid is made by pressing together a mixture of powders composed of oxides containing ferric ions. The magnetic properties arise from the interaction between metallic ions and oxygen ions in the crystal structure of the oxide. By mixing divalent metal ions such as Mn, Co, Ni, Cu, Mg, and Zn in the compound, properties can be tailored for a variety of short-pulse induction accelerator cell designs.

The solid state physics issues of ferrites are covered extensively in many textbooks [2–5]. The two most common ferrites are nickel–zinc (Ni–Zn) and the manganese–zinc (Mn–Zn). The resistivity of the Ni–Zn ferrites is in the range of 10^4–10^7 Ω-cm and for Mn–Zn it is in the range of 10–10^4 Ω-cm. The flux density swing for the Ni–Zn is 0.7 T and for Mn–Zn it can exceed 1.2 T. The relative permeability for both ferrites is in the range of 10–10^4 and the permittivity is typically about 10 but can be as high as 10^5 in some low conductivity Mn–Zn ferrites.

The properties of the Mn–Zn ferrites appear to be a good choice for medium pulse duration in transitioning from short-pulse to long-pulse since they offer twice the flux density of the Ni–Zn. However, because some of the higher flux density Mn–Zn ferrites have several orders of magnitude lower resistivity, they have much greater losses than the Ni–Zn ferrites at high frequencies. Besides the eddy current losses, another effect has been observed in Mn–Zn ferrites called dimensional resonance [6]. Associated with the low resistivity of the Mn–Zn ferrites there is an effective permittivity (ϵ_r) which can be as high as 10^5. Analytical studies have been made for typical Mn–Zn ferrites and the resonances have been calculated. The high value of permeability and permittivity give rise to standing waves within the ferrite. Under these conditions the measured permeability drops to near zero. This occurs when the smallest dimension of the cross section perpendicular to the electric field equals half a wavelength. Mn–Zn ferrites have not been used in induction cells for the above mentioned reasons and also because great advances have been made in thin ribbon metallic magnetic materials which can be used at any pulse duration depending on the actual accelerator requirements.

The maximum flux swing for ferrites is set by the crystal structure and there is little that can be done to change it. The resistivity of 10^6 Ω-cm or larger leads to negligible eddy current losses even with very short pulses. The property which can be most affected by variations of the divalent metal ions Ni–Zn is the permeability or ferromagnetic resonance frequency. By reducing the nickel content and replacing it with zinc, the relative permeability can be increased from 10 to 10^4. The higher the permeability the lower will be the spin resonance or the point where the ferrite losses begin to dominate. Figure 5.1(A–E) shows that if the compositional ratio of Ni/Zn is increased, the spin resonance goes from 1–100 MHz and the real part of the permeability [7] goes from 1,000 down to ten. In an induction accelerator it is desirable to have a high permeability to reduce the nonlinear portion of the magnetizing current. The composition of the ferrite can actually be tailored to a

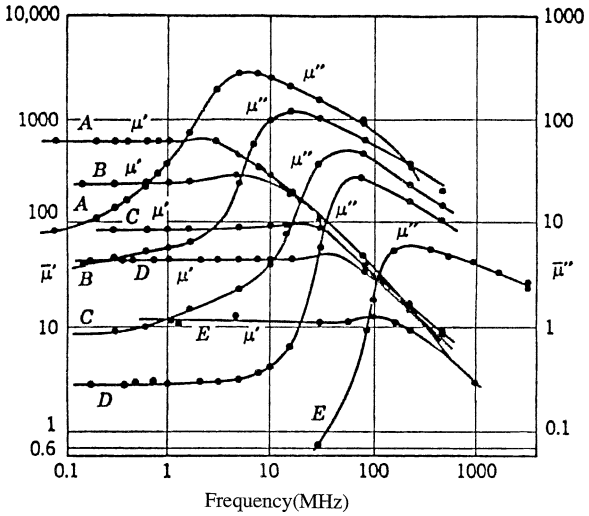

Fig. 5.1 Frequency dependence of real and imaginary parts of permeability for Ni–Zn ferrite as Zn is substituted by Ni from A–E

defined pulse duration so that the optimum pulse can be achieved with very low losses as was done with the Advanced Test Accelerator (ATA).

Figure 5.2 shows the hysteresis loop of PE11B, a Ni–Zn ferrite which was used in the ATA accelerator. This ferrite was developed by TDK for this specific application and required ~500 A-turns per meter of magnetizing current to achieve the full flux swing. The energy density losses, $U = (1/2)BH$ J/m^3, can be obtained by integrating the forward hysteresis loop from $-B_r$ to $+B_r$, where B_r is the remnant flux at zero coercive force ($H_c = 0$). A low level pulse of much longer duration and of opposite polarity to the main pulse is applied to reset the core from $+B_r$ to $-B_r$. For PE11B ferrite the energy density loss with a 100 ns saturation pulse is about 120 J/m^3.

The selection of ferrites instead of ferromagnetic materials for pulse durations less than 100 ns is not a firm criterion. It depends on many factors determined by the accelerator requirements such as current, efficiency, gradient, power dissipation and cost. A design example in the next chapter will show that if efficiency is important, ferrites may well be the right choice. If Ni–Zn ferrites are the optimum choice, a guideline which has been used in several previous accelerators is that the fundamental frequency of the pulse is at or near the spin resonance (see Sect. 3.7). This insures that the permeability is still high and the losses are low for the duration of the pulse.

Although core losses for Ni–Zn ferrites are relatively low, in high repetition rate accelerators cooling will be required to keep the temperature rise below certain limits. The flux swing decreases with temperature and improper cooling can lead to runaway conditions if the magnetic material temperature approaches the Curie point where the flux density approaches zero. More will be said on this issue in Sect. 6.11 discussing cell losses and cooling.

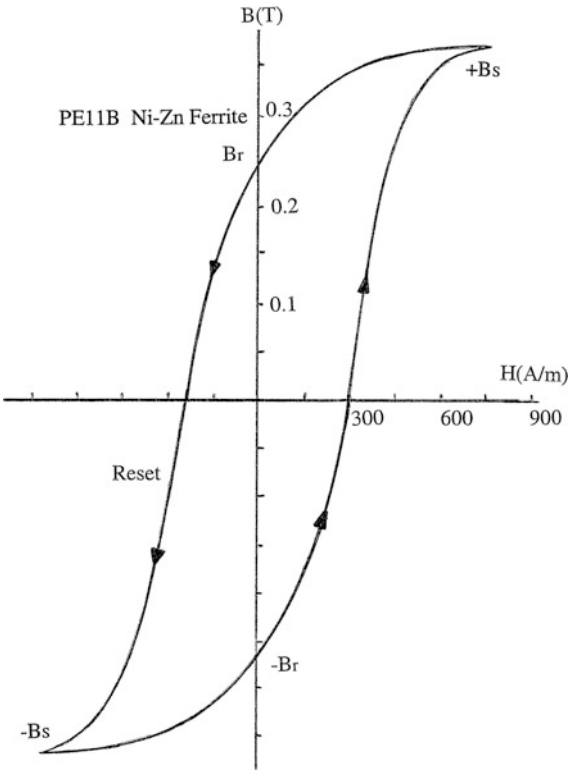

Fig. 5.2 Hysteresis loop for PE11B Ni–Zn ferrite with a saturation time of 100 ns

5.3 Ferromagnetic Materials

For long-pulse applications, the cross-section(volume) of the cell using ferrite becomes impractically large and leads to very low accelerating gradients. A magnetic material with much greater flux swing is required to make the design practical. All the ferromagnetic materials have flux swings two to five times greater than the nickel–zinc ferrites but all have resistivities many orders of magnitude lower. As it is well known, a changing magnetic flux in a conductive medium will induce eddy currents in that medium which will result in energy loss. The magnitude of that loss depends on the rate of change, the resistivity, the permeability and most importantly the shape or size of the conductive medium. As in the case of the first induction accelerator, the Astron, the only way to reduce the losses and make the ferromagnetic nickel-iron (Ni–Fe) practical for the induction cell is to subdivide the core material into very small electrically insulated regions or laminations [8]. In the early 1960s the manufacturing of these cores with 25 μm insulated ribbon required considerable development and was very costly. During the last three decades, researchers have developed a new class of magnetic materials called metallic glasses and nanocrystalline metals that are manufactured by various companies

under different trade names. These materials have high flux swing, low magnetization fields and a higher resistivity than the well known ferromagnetic materials and they can easily be manufactured as a very thin ribbon 15–40 μm thick [9–13].

The development of these materials was initially driven by the energy saving potential of the 60 Hz power distribution system. Since the primary windings of the distribution transformers are always connected to the power grid, the magnetic material continuously cycles around the hysteresis loop at power line frequency draining a small but not insignificant fraction of the power and turning it into heat. It was estimated in the early 1980s that over 10^{10} kW-h could be saved in the United States in one year if all of the transformers in usage could have been replaced by amorphous magnetic material. This incentive drove a number of companies in the US, Japan and Europe to develop manufacturing techniques that could produce very large quantities of the thin ribbon at very low cost from inexpensive alloys. Initial research on the amorphous metals can be attributed to several universities and corporations, but the composition of many alloys and the development of Metglas production techniques that revolutionized the manufacturing process were led by Allied Corporation. There are several techniques for producing an amorphous phase metal, but the most common is melt spinning where the alloy is ejected onto a cold, rapidly rotating wheel by a nozzle up to a few tens of centimeters wide. The ribbon thickness of 15–40 μm is controlled by adjusting the proximity of the nozzle to the wheel. The rapid cooling of the melt at greater than 10^5°C/s avoids crystallization and the amorphous alloy is created at very high speeds (tonnes/hour). The term metallic glass appears to be contradictory but the structure of these amorphous materials does resemble that of glass and their electrical conductivity is much like that of ferromagnetic metals.

The amorphous alloys have found applications in nonlinear pulse compression modulators, induction accelerators and many other areas requiring thin ribbon [14, 15]. Magnetic materials for pulse applications are subjected to very high rates of magnetization where dB/dt can exceed 10 T/μs. In comparison, the magnetization rates at 60 Hz are four to five orders of magnitude lower. This is a relevant difference because the voltage generated for each layer of ribbon is in the hundreds of microvolts at 60 Hz and can be in the tens of volts for pulsed applications. The significance of this difference is that for applications at 60 Hz the surface resistance between layers is sufficiently high to block eddy current flow without additional insulation. For pulse applications with tens of volts between layers, the resistance is not sufficient to block current flow and additional insulation is required to isolate the individual layers. Without insulation between layers excessive eddy currents would render the magnetic material useless.

During the development of the amorphous alloys for the 60 Hz industry, it was found that the as-cast magnetic properties were not very desirable for transformers regardless of cost. In order to achieve the required high flux swing, low coercive force and high permeability, the material had to be field annealed. That is, the material was cast and wound into a core, a circumferential field was applied and the temperature was raised to 300–400°C. Figure 5.3 shows the hysteresis loops for the as-cast and for the field-annealed metallic glasses. It was concluded that for these

alloys to be competitive with existing materials transverse field annealing would be required.

Recalling that for pulsed applications many volts can appear between layers, studies to provide additional inter-laminar insulation of annealed cores were initiated. One option for achieving the optimized properties in pulse applications was to field-anneal prior to winding the core with additional insulation between ribbon layers. Unfortunately, annealing of most alloys embrittles the material to such an extent that it becomes very difficult to wind into a core and the labor intensive winding process eliminates all cost advantages. Some annealed alloys such as 2605CO have been successfully wound into large cores but in these particular applications cost and energy loss were not deciding factors. Coatings that withstand annealing temperatures have been successfully developed by several companies and are becoming more cost competitive with the as-cast material [16–18]. At the time of the design studies of heavy ion fusion and for DARHT-II, tests made on magnetic materials with commercial coatings for inter-laminar insulation offered inconsistent results. Some of the magnetic properties had deteriorated and inter-laminar shorts developed that made the application of this coating technique a very risky proposition. In the last several years, inter-laminar insulation that holds off several volts has proven to be reliable and economically viable but not yet cost competitive with the as-cast material. Since the cost difference between the as-cast and the annealed materials was not acceptable for the heavy ion and the DARHT-II accelerators, it was essential to determine if the as-cast material offered a viable solution simply by winding the ribbon with 2.5 μm Mylar as inter-laminar insulation.

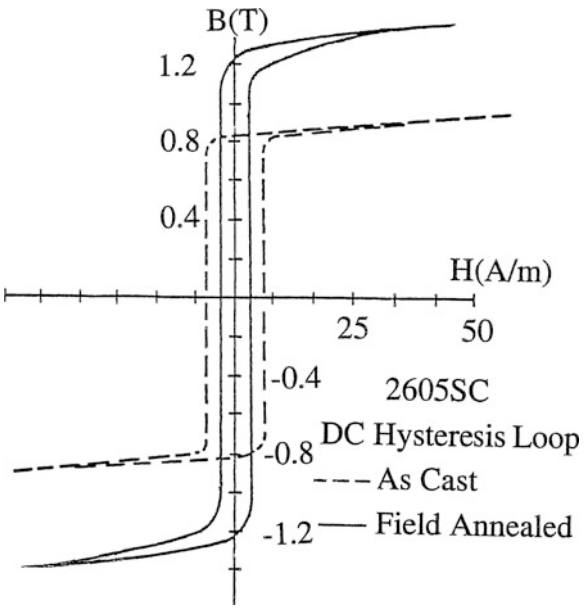

Fig. 5.3 Hysteresis loops for as-cast and field-annealed 2605SC

5.4 Energy Loss

The dominant loss mechanism in ferromagnetic ribbon at high magnetization rates is basically due to the eddy current losses (see Sect. 6.9 for a discussion of the electromagnetic fields and the eddy currents in a ferromagnetic ribbon core). A full description of the dynamics of all magnetization losses is more complicated, but for rates above about one T/μs a model sometimes referred to in the literature as the "saturation wave theory" has proven useful in showing how the losses scale with magnetization rate, ribbon thickness, etc. This theory models the major components of the excitation losses in terms of the eddy currents within the magnetic ribbon and the time required for the field to fully penetrate. In this model the coercive field, H_a, required to fully magnetize the material from $-B_r$ to $+B_s$ is given by

$$H_a = H_c + \frac{d^2}{8\rho}\frac{\Delta B}{2B_s}\frac{\mathrm{d}B}{\mathrm{d}t}, \tag{5.1}$$

where H_c is the DC coercive field, $\Delta B = B_r + B_s$, and d and ρ are the ribbon thickness and resistivity respectively. The half cycle energy density $\mathcal{E}$ lost in magnetizing the core to B_s is:

$$\mathcal{E} = H_c \Delta B + \frac{d^2}{8\rho}\frac{\Delta B^2}{2B_s}\frac{\mathrm{d}B}{\mathrm{d}t}, \tag{5.2}$$

where the first term ($H_c \Delta B$) is the DC anisotropy energy and the second term represents dynamic (eddy current) losses which dominate at high magnetization rates [19, 20]. To accurately quantify the magnetic material losses at high $\mathrm{d}B/\mathrm{d}t$ rates, the hysteresis curve is always measured at those rates and the energy loss per unit volume (J/m^3) is obtained by integrating the area under the B–H loop [19, 21]. It is evident from Eq. (5.1) that the coercive field, H_a, is proportional to the magnetization rate and the ribbon thickness squared but inversely proportional to the resistivity.

To evaluate the benefits of annealing when operating at high magnetization rates, hysteresis loop measurements of large as-cast amorphous cores of 2605SC were made with $\mathrm{d}B/\mathrm{d}t = 1$ T/μs. These measurements show that unlike the 60 Hz results taken at very low magnetization rates the saturation flux, B_s, is nearly the same as that of the annealed cores. Figure 5.4 shows the hysteresis loop for the as-cast 2605SC at 2 μs saturation time. The losses per unit volume are about the same as the annealed material but the hysteresis loop is more S-shaped, so more compensation is required to maintain constant voltage during the pulse. The remanent flux is also lower which leads to lower flux swing from $-B_r$ to $+B_s$. This reduction in flux swing, however, can be avoided by maintaining a reset current flow just prior and during the forward pulse ("active reset"). This reverse current flow is typically a pulse of much longer duration and orders of magnitude lower power than the main pulse, but still sufficient to bias the core near $-B_s$ instead of $-B_r$. This gains back most of the $(B_s - B_r)$ that would be lost without the use of this "active reset".

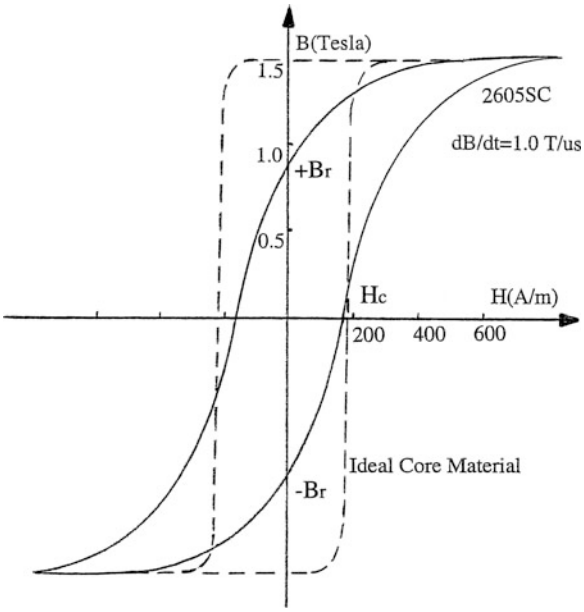

Fig. 5.4 Hysteresis Loop for 2605SC amorphous material

A clear advantage of the annealed amorphous or nanocrystalline materials is that the hysteresis loop approaches the squareness of the ideal material shown in Fig. 5.4. Although the overall losses may be comparable to the as-cast material, the compensation network to achieve constant voltage during the pulse is much easier, or not required, since the magnetizing current is constant (time independent).

In the material selection process the different trade offs need to be evaluated. As previously mentioned, for 60 Hz operation, field annealing of the as-cast amorphous ribbon is essential in order to obtain full saturation flux with low magnetization or coercive field. Although it was believed initially that annealing would also be required for applications with high magnetization rates, the as-cast material offered more than satisfactory performance. This made the DARHT-II accelerator economically feasible since coatings that could withstand annealing were unreliable or prohibitively expensive at that time.

Empirically obtained loss data for annealed and as-cast materials are shown on Fig. 5.5. The losses and measured flux swing at high magnetization rates are quite comparable. Several alloys and Ni–Zn ferrite are shown on this chart. The alloy 2605CO, which could be wound after annealing, shows more than twice the losses of the as-cast 2605SC and also costs considerably more due to the cobalt content. Note that the PE11B ferrite losses are approximately an order of magnitude lower than 2605SC and do not become significant until $\mathrm{d}B/\mathrm{d}t$ is above 10 T/μs. There are several alloys such as 2705M and 2714 that have losses lower than 2605SC but their flux swing is considerably less and their cost is greater. These alloys should

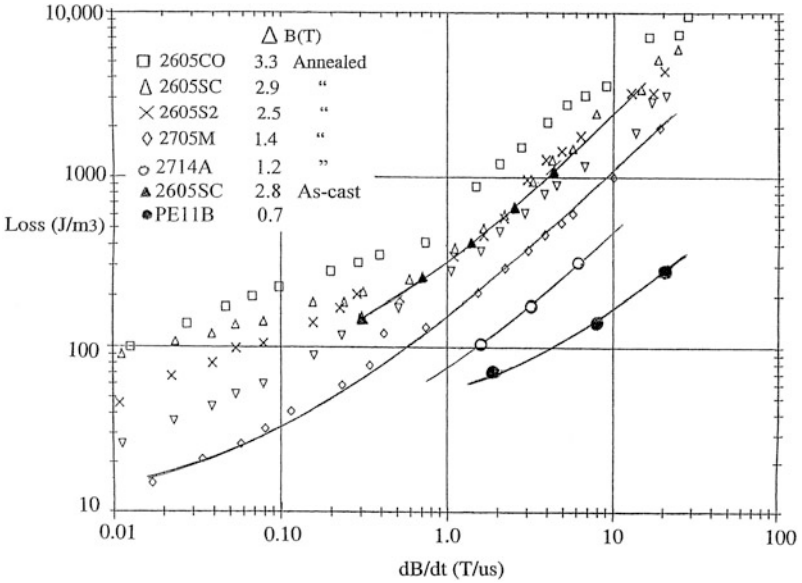

Fig. 5.5 Magnetic material losses versus magnetization rate

definitely be considered in cell designs where high efficiency is required and low cost is not the deciding factor [20, 22].

The discussion of energy loss in this section has concentrated on the case where the full flux swing of the magnetic material is utilized, since that minimizes the material cost for a given pulse length and core voltage. At very high repetition rates, however, the optimum design choice may lead to situations where only a fraction of the available flux swing is used . This case is discussed in Chap. 11, where it is shown that the magnetization energy loss with a minor hysteresis loop has a different scaling than presented in Eq. (5.2).

5.5 Other Materials

The discussion on ferromagnetic materials for long-pulse accelerators has concentrated mainly on amorphous metals since in the past they were readily available and offered a viable solution to achieving the technical requirements at a reasonable cost. The fact that the amorphous metals have similar flux swing to the nickel–iron or silicon steel, have a higher resistivity and can be mass produced in thinner and wider ribbon by very low cost manufacturing techniques make them the compelling choice for long-pulse accelerators and many other applications where large quantities are needed.

Over the last decade, the cost of some amorphous metals dropped nearly one order of magnitude making the DARHT-II long-pulse accelerator economically

viable. Studies of induction linac accelerators to drive a heavy ion fusion power plant (see Sect. 10.1) estimate that over 10^7 kg of magnetic material would be required and to make the linac economically feasible the cost would have to decrease by nearly another order of magnitude. There are many other applications for induction cells such as induction synchrotrons, recirculating linacs, relativistic two beam accelerators for microwave generation, linacs for food processing and muon phase rotation where the material's cost is not a major driving factor. In these cases, the cell designer has considerable latitude in the material choices, and this allows the final selection to be based primarily on the cell performance and not cost.

There are several manufacturers that produce a variety of materials by various techniques that are competitive in both magnetic properties and cost with the amorphous alloys Metglas. Hitachi Metals Ltd. (Japan) has developed a number of alloys that have comparable properties to the amorphous metals. These alloys, including Finemet, are produced as a nanocrystalline material by adding small fractions of copper and Niobium. Some of these alloys have lower losses than the amorphous metals and are currently being manufactured as complete cores with sufficient inter-laminar insulation on the ribbon to be applicable at high magnetization rates. Although still not cost competitive with the as-cast alloys, these cores have found extensive usage in induction synchrotrons, step-up transformers and nonlinear pulse compression modulators. There are other magnetic materials that are produced as a thin ribbon by various methods in several countries. Vitroperm is an alloy similar to Finemet manufactured by Vacuumschmelze (Germany) and Moscow Radio Technical Institute (MRTI-Russia) also produces many comparable amorphous materials [23–27].

Extensive material studies were undertaken by Molvik and Faltens for the heavy ion fusion application since the induction cells would be a major cost factor for inertial fusion accelerators. Many small cores from several different manufacturers were tested and all the magnetic properties such as flux density, coercive field, losses at different magnetization rates and other issues such as coatings and annealing were investigated. Table 5.1 below shows a small data sample from that report for coated/annealed materials [28–30].

The sample data shows that the amorphous materials 2605SA1 and 2605SC have losses approximately twice those of the nanocrystalline materials which have slightly lower flux density. This report describes in detail the progress which has been made in the last decade. The coating/annealing process seems to have been

Table 5.1 Sample data from [28–30]

Material @ $dB/dt = 1$ T/μs		ΔB [T]	$\mathcal{E}$ [J/m^3]
Metglas	2605A1	2.2	350
	2605SC	2.4	400
Finemet	FT-1H	2.1	150
	FT-2H	2.4	200
Vitroperm	NAM-2	2.2	150
	NAM-3	2.1	120
MRTI	2605A1	2.1	300
	2605SC	2.2	400

satisfactorily resolved and future cores with improved magnetic properties will be readily available from several different manufacturers. Clearly, advancements have been made and will continue to be made but an important point which should not be lost about the as-cast amorphous alloys is that their magnetic properties at high magnetization rates are comparable to the annealed materials and at the time of the DARHT-II design the cores were available at one fifth the cost. It has yet to be established if in the future the new and improved annealed materials with sufficient inter laminar insulation for high magnetization rates will be cost competitive with the as-cast [30].

5.6 Summary

There are several manufacturers of ferrite in the US, Europe and Asia that offer many types of ferrites that are competitive in quality and prices to those mentioned in the text. The induction cell designer should investigate and compare the magnetic properties of all available materials to assess their impact on the complete system. It may well be that if a more expensive material with lower losses and a square hysteresis loop is used, it could lead to a simpler pulse generator and compensation network and ultimately result in better performance and overall lower cost. After reviewing the performance data of available materials, it is advisable to test many samples under the same conditions as the specific application for which they are intended. Once the parameters are well characterized, the cell designer can choose the magnetic material to meet all technical and economic goals be it ferrite, amorphous or nanocrystalline. The cell designer should evaluate and eliminate any weak points, and maximize the safety factors that influence the future performance of the cells particularly if they are produced in large quantities. Events such as deterioration of magnetic properties due to mechanical stress, deterioration of inter-laminar insulation due to pulsing or movement and deterioration of voltage holding caused by improper impregnation of the insulating medium must also be carefully considered. The final prototype cell should then be tested at elevated levels well above the normal operating level to insure that the final design will give reliable performance for the desired life expectancy of the accelerator.

References

1. A. Faltens and E. Hartwig. Preliminary Hardware Concepts for an Electron Ring Accelerator. *IEEE Trans. Nucl. Sci.*, NS-18:484–487, 1971. (Proceedings of the 1971 Particle Accelerator Conference, Chicago, IL, 1–3 Mar., IEEE-NPSS).
2. C. Kittel. *Introduction to Solid State Physics*, Wiley, New York, NY, 8th edition, 2005.
3. E. Snelling. *Soft Ferrites: Properties and Applications*, Butterworth, London, 2nd edition, 2000.
4. J. Smit and H. Wijn. *Ferrites*, Wiley, New York, NY, 1959.
5. R. Bozorth. *Ferromagnetism*, D. Van Nostrand Co. Inc., New Jersey, 1951.
6. F. Brockman. Dimensional Effects Resulting from High Dielectric Constant Found in a Ferromagnetic Ferrite. *Phys. Rev.*, 77:85, 1950.

7. E. Gorter. Magnetization in Ferrites: Saturation Magnetization of Ferrites with Spinel Structure. *Nature*, 165:798, 1950.
8. S. Winter, R. Kuenning, and G. Berg. Pulse Properties of Large 50–50 Ni–Fe Tape Cores. *IEEE Trans. Magn.*, 6:41–45, 1970.
9. R. O'Handley, S. Murray, and S. Allen. Low-Field Magnetic Properties of Fe80B20 Glass. *J. Appl. Phys.*, 47:4460, 1976.
10. F. Luborsky. Perspective on Applications of Amorphous Alloys in Magnetic Devices. In R. A. Levy and R. Hasegawa, editors, *Amorphus Magnetism II*, page 345, Plenum Press, New York, NY, 1977.
11. A. Glaser and R. Tagirov. Amorphous Magnetic Materials. *Acad. Sci. USSR Phys. Ser.*, 42–48:1600, 1978.
12. P. Chaudhari, B. Giessen, and D. Turnbull. Magnetic Glasses. *Sci. Am.*, 242:98, 1980.
13. L. Davis, N. de Cristofaro, and C. Smith. Technology of Metallic Glasses. In *Proceedings of the Conference on Metallic Glasses: Science and Technology*, page 125, Budapest, Hungary, 30 June–4 July 1980. Springer, The Netherlands.
14. C. Smith. Metallic Glasses for Magnetic Switches. In *Proceedings of the 15th Power Modulator Symposium*, page 22, Baltimore, MD, 14–16 June 1982.
15. C. Smith. Magnetic Shielding to Multi-Gigawatt Magnetic Switches: Ten Years of Amorphous Magnetic Applications. *IEEE Trans. Magn.*, MAG-18:1376, 1982.
16. C. Smith, B. Turman, and H. Harjes. Insulations for Metallic Glasses in Pulsed Power Systems. *IEEE Trans. Electron Devices*, 38:750, 1991.
17. A. Molvik, W. Meier, R. Moir, and A. Faltens. Implications of New Induction Core Materials and Coatings for High Power Induction Accelerators. In *Proceedings of the 1999 Particle Accelerator Conference*, pages 1503–1505, New York, NY, 29 Mar.–2 Apr. 1999.
18. C. Smith, A. Faltens, and S. Rosenblum. Insulation for Metallic Glasses in Pulse Power Systems. *J. Appl. Phys.*, 57:3508, 1985.
19. R. Jones, A. Collins, and N. Cleaver. A Comparison of the Step $\mathrm{d}B/\mathrm{d}t$ Pulse Magnetization Losses in Some Amorphous Ribbon and Conventional Toroids. *IEEE Trans. Magn.*, MAG-17:2707, 1981.
20. C. Smith and D. Nathasingh. Magnetic Properties of Metallic Glasses Under Fast Pulse Excitation. In *Proceedings of the 16th Power Modulator Symposium*, page 240, Arlington, VA, 18–20 June 1984. IEEE, New York, NY.
21. R. Jones. Step $\mathrm{d}B/\mathrm{d}t$ Magnetization Losses in Toroidal Amorphous Ribbon and Polycrystalline Cores. *IEEE Trans. Magn.*, MAG-18:1559, 1982.
22. C. Smith and L. Barberi. Dynamic Magnetization of Metallic Glasses. In *Proceedings of the 5th IEEE Pulse Power Conference*, page 664, Arlington, VA, 10–12 June 1985. IEEE/NPSS.
23. Y. Yoshizawa, S. Oguma, and K. Yamauchi. New Fe-Based Soft Alloys Composed of Ultrafine Grain Structure. *J. Appl. Phys.*, 64:6044, 1988.
24. S. Nakajima, S. Arakawa, Y. Yamashita, and M. Shiho. Fe-Based Nanocrystalline FINEMET Cores for Induction Accelerators. *Nucl. Inst. Meth. A*, 331:5556, 1993.
25. G. Mamaev, I. Bolotin, A. Ctcherbakov, and S. Mamaev. Fe-Based Nanocrystalline FINEMET Core for Induction Accelerators. In *Proceedings of the 1997 Particle Accelerator Conference*, page 1313, Vancouver, Canada, 12–16 May 1997.
26. S. Nakajima, S. Arakawa, Y. Yamashita, and M. Shiho. Fe-Based Nanocrystalline FINEMET Core for Induction Accelerators. *Nucl. Inst. Meth. A*, 331:318, 1993.
27. S. Vonsovskii and E. Turov. Metallic Glasses and Amorphous Magnetism. *Acad. Sci. USSR Phys. Ser.*, 42:1570, 1978.
28. A. Molvik and A. Faltens. Induction Core Alloys for Heavy-Ion Inertial Fusion-Energy Accelerators. *Phys. Rev. Spec. Topics Accl. Beams*, 5:080401, 2002.
29. R. Hasegawa. Properties and Applications of Nanocrystalline Alloys from Amorphous Precursors. *NATO Sci. Ser.*, 184:189–198, 2006.
30. R. Wood and R. Lathlaen. Amorphous Material Coatings. In *Proceedings of the 12th Pulsed Power Conference*, page 1313, Monterey, CA, 27–30 June 1999.